COBEM 2023 27TH INTERNATIONAL CONGRESS OF MECHANICAL ENGENEERING

ABCM Brazilian Society of Mechanical Sciences and Engineering
27th ABCM International Congress of Mechanical Engineering
December 04-08, 2023, Florianópolis-SC, Brazil

COB-2023-2359
BIO-INSPIRED SMALL WIND TURBINES USING FLYING SEEDS GEOMETRY

Bruno Fracaro Cid de Alcantara
Ramiro Bertolina
Universidade de Brasília, Department of Mechanical Engineer, Laboratory of Energy and Environment, 70910-900 Brasília, DF, Brazil
bruno.fracaro.alcantara@gmail.com
ramirodematosbertolina@gmail.com

Antonio Brasil Junior
Universidade de Brasília, Department of Mechanical Engineer, Laboratory of Energy and Environment, 70910-900 Brasília, DF, Brazil
brasiljr@unb.br

Abstract. *This research paper investigates the power coefficient of falling seeds from the Pterogyne nitens tree and aims to develop a small wind turbine with blades inspired by the seed's wing-shaped geometry. The study explores the seeds' geometry, structure, fibers, weight, surface characteristics, and flight dynamics to understand their motion and potential for energy generation. High-speed cameras were used to capture the seed's position and inclination during laboratory tests, which provided parameters for rotation and descent. The results align with previous research, indicating that the falling seed from this species achieves a power coefficient of over 35%. These findings offer insights into the potential for biomimicry in wind turbine design and highlight the importance of understanding natural systems for sustainable energy solutions. This research paper presents a study on various turbine models aimed at optimizing the blades and evaluating the power coefficient obtained. Numerical analysis was performed on ANSYS CFX software with the Shear Stress Transport turbulence model and a mesh model designed to accurately reflect the blade/fluid interface and the turbine wake. Several turbine designs were evaluated, varying characteristics such as blade size, pitch angle, and blade surface. The designed blades showed significant differences from traditional models, with an aspect ratio of 4.2 (as opposed to the conventional of over 10) and a larger chord length near the tip of the blade. The blades were tested as flat surfaces, enabling the study of the surface geometry rather than the wing profile. CFD results showed a power coefficient of 0.26 for the proposed turbine model. Further studies are required to improve the power coefficient extracted by the turbine, including experimenting with different aerodynamic profiles.*

Keywords: *Small wind turbines, Flying Seeds, Numerical Modeling with CFD*

1. INTRODUCTION

The current generation of wind turbine development has been directed toward larger and larger turbines, capable of producing up to 15 MW of power and blade lengths of over 100 meters (Gaertner *et al.*, 2020). While this made it possible for great power generation with a single turbine, it also posed obstacles to the construction of wind farms. The cost of transportation and installation heavily impacts the cost of the wind farm (LJ *et al.*, 2006), and the incapability to transport the turbine to some locations means that areas with good wind conditions could stay unused.

On the other end of this spectrum, distributed energy generation (DEG), when energy is generated at a small or medium scale close to the location of usage, is increasing in relevance, with projections showing an increase of 380% by 2030 (IEA, 2022). Small horizontal axis wind turbines (S-HWAT), defined by Sathyajith and Philip (2011) as "having a rotor swept area (equal to $\pi \times R^2$ where R is the radius of the blade tip) of less than 200 m²", play a major role in DEG, and the pursuit of higher efficiency models represents a prominent research trend worldwide.

S-HAWTs are commonly associated with lower efficiency compared to their larger counterparts in terms of power output relative to available power (Sathyajith and Philip, 2011). Several factors contribute to this lower efficiency. One key factor is the less favorable flow conditions near the ground. The average wind velocity at ground level is significantly slower, and the presence of obstacles such as trees and structures introduces higher turbulence, which is detrimental to wind turbine operation. Moreover, small turbines operate at lower Reynolds numbers, typically around 1.2×10^3, whereas larger turbines operate at expected Reynolds numbers over 5×10^5. This discrepancy in Reynolds numbers has a substantial impact on turbine performance.

In order to learn how to better use the flow conditions at the conditions near the ground, it is wise to analyze and take inspiration from whom have been adapting to these circumstances for millions of years, nature. This concept, referred to

as Biomimetics, is not new and has been seen in the past, especially regarding aerodynamics. Bird wings have inspired the development of wing designs for aircraft that offer improved aerodynamic performance. By studying the shape, structure, and flexibility of bird wings, engineers have developed wing designs with better lift-to-drag ratios and enhanced maneuverability. In recent years, the field of turbine development has witnessed extensive research focusing on various approaches for turbine blade design. One study conducted by Ikeda *et al.* (2018) explored the development of turbine blades inspired by bird wings, with particular emphasis on replicating the wing flex characteristics.

In the matter of extracting wind power, several trees have developed mechanisms to harvest the wind power and increase the area of dispersal of its seeds, a vital function for the species' survival. These mechanisms often came in the form of winged seeds. The winged seeds, referred to as samaras, are a category of seed that has a fibrous membrane extending from the seed, in the shape of a wing. When the samaras are released from the tree, their wing and weight distribution promote a self-rotation during the fall that strongly resembles the motion of an S-HAWT. This motion, allied with the geometry of the samaras, produces a lift for the samara, reducing its falling velocity, and maintaining the samara gliding through the air even at no wind conditions.

The gliding behavior of falling samaras has been extensively studied in various research works. Azuma and Yasuda (1989) measured and then tested ten species of samaras in a vertical wind tunnel, obtaining the flight parameters and performance of the studied samaras. Arranz *et al.* (2018) defined a generic winged seed geometry and constructed a corresponding CAD model, the researcher then employed Direct Numerical Simulations (DNS) to simulate the flow around the falling seed model and analyze its characteristics. It is also believed that these samaras exhibit a power coefficient that approaches the theoretical limit for wind turbines, as highlighted by Holden *et al.* (2015), which encourages the development of a bio-inspired turbine model. While the most commonly studied samaras are derived from maple tree species found in the northern hemisphere, this study focuses on analyzing the samaras of the *Pterogyne nitens*, a tree species indigenous to the biome in which the Universidade de Brasília is situated. The samaras of *Pterogyne nitens* are depicted in Figure 1. The wing section geometry of these samaras will serve as the basis for developing the turbine blades.

Figure 1: Specimens of samaras from *Pterogyne nitens* trees.

For the development of wind turbines, simulations conducted using Computational Fluid Dynamics (CFD) software offer the most effective approach for the development of wind turbine models. CFD simulations provide a detailed understanding of complex aerodynamic phenomena involved in wind turbine operation such as flow separation, blade stall, and wake effects. By numerically solving the governing equations that describe fluid flow and turbulence, CFD software allows for accurate prediction and visualization of airflow patterns and calculation of the expected power coefficient of the turbine for the given flow conditions. The simulation of HAWT on CFD software has been strongly covered by the literature, showing great correspondence between the simulated model and the real-life device when performed properly. In this study, we perform multiple simulations on ANSYS CFX following proven methods presented in Section 2.

This study aims to analyze the falling of a samara of the *Pterogyne nitens* tree and develop a wind turbine with blade geometry that strongly resembles the geometry of the samaras. The samara will be analyzed regarding its geometrical characteristics and flight parameters, using techniques that shall be discussed in the methodology section. The proposed turbine models will be built using CAD software and tested through CFD simulations, regarding mainly its produced torque and power coefficient. Multiple turbine models will be built to assess the influence of parameters such as blade number and pitch angle, the goal is to produce an efficient model of a bio-inspired small wind turbine and obtain its power coefficient curve.

2. METHODOLOGY

2.1 Flight parameters of falling samaras

Various *Pterogyne nitens* samaras specimens were collected to perform flight experiments in a controlled environment. The geometrical characteristics of these specimens are shown in Table 1 below:

Comparing the *Pterogyne nitens* values to those of maple seeds studied by Azuma and Yasuda (1989), we observe that *Pterogyne nitens* samaras are longer in length but have a smaller aspect ratio and weigh less. The specimens have an 8% standard deviation of the average, so we can consider the specimens uniform in their geometrical characteristics, this is favorable to designing a blade with the samara geometry as the blade will be approximate to the samara geometry.

	Minimum	Maximum	Average	Standard Deviation
Length (mm)	40	51	44.1	4.25
Max Width (mm)	10	13.6	12.5	1.44
Weight (g)	0.0882	0.1381	0.1240	0.0206
Aspect Ratio	3.2	4.2	3.56	0.41
Max thickness (mm)	2.5	2.88	3.56	0.43

Table 1: Geometry of the specimens collected

To determine important flight parameters, the samaras were released from a measured height of 2.5 meters. The parameters were measured at the bottom 0.5 meters of the glide, in an area with no wind. For the measurements, it was used a high-speed capturing camera, capturing at 960 frames per second, allied with a computer program to measure the samara position at each frame at a given time. The data collected from the experiments are shown in Section 3:

2.2 Samara scanning and development of turbine CAD models

To precisely represent the samaras geometry in a CAD model, the specimens were scanned using a structured light technique with the David SLS-3 scanner, and photogrammetry of the subject, these made it possible to build the turbine blades with great fidelity to the samaras geometry. Figure 2 shows the CAD blade model compared to the samara.

(a) (b)

Figure 2: (a) A photo of the samara. (b) The CAD model of the samara.

The turbines were designed at a scale model around a 41 mm diameter hub with a half sphere with the same diameter as the nose. This hub was selected for being previously used in other studies by the university Brasil Junior *et al.* (2017), so its effects on the flow are well known. The turbine blades consist of the wing area of the samara. Only the wing area was considered for the blades due to the fact that the seed area does not produce lift for the samara during its falling. The turbine blades were built 2.5 times larger than the actual samaras. This option was made in order to match the seed area to the hub area, making the samara wing the turbine blade. The resulting diameter of the turbines is 206 mm. Multiple turbine models were developed varying their characteristics as the number of blades and pith angle, and evaluated by their power coefficient, as will be discussed further. The turbine model with 8 blades and a 30° pitch angle is shown in Figure 3 below:

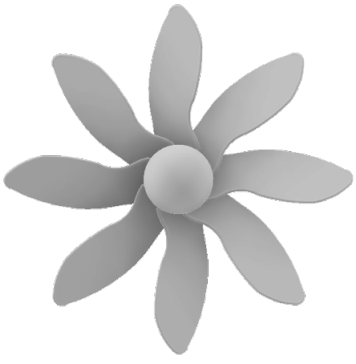

Figure 3: CAD image of the second generation turbine.

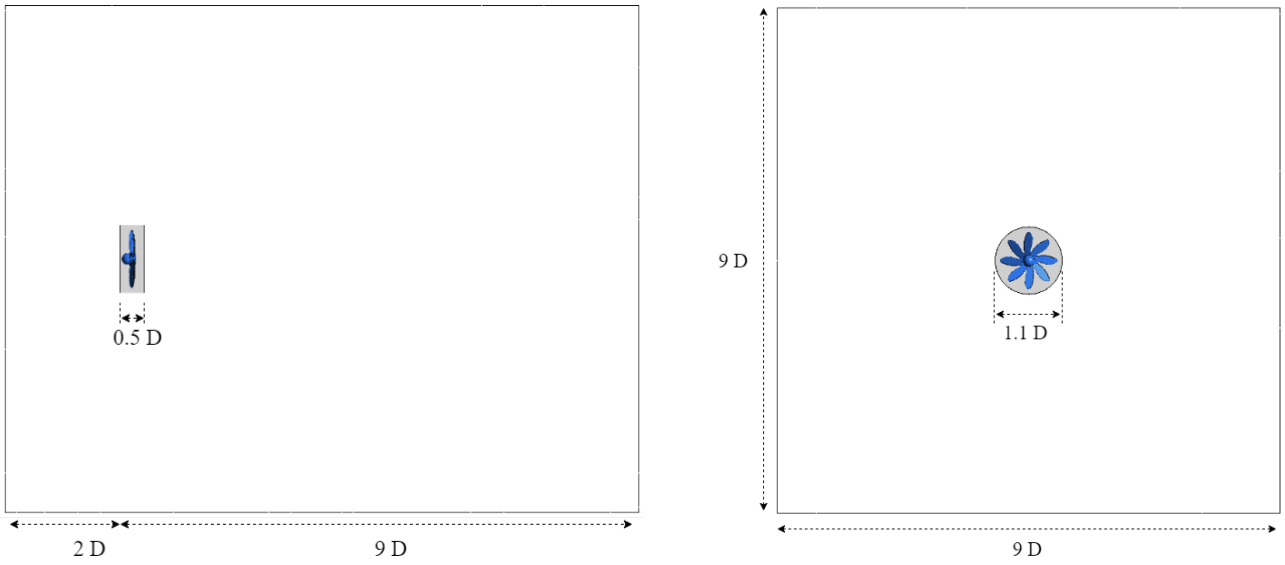

(a) (b)

Figure 4: (a) Side view of the domains and turbine. (b) Front view of the domains and turbine.

2.3 CFD simulations, mesh generation, and solver setup

In order to evaluate the power coefficient of the proposed turbine models in different configurations, CFD simulations were conducted using the Ansys CFX software. The simulation setup was designed to follow the methodology outlined by Brasil Junior *et al.* (2017) but using larger domains and is described in detail here. The turbine was positioned within a cylindrical rotating domain, which had a radius of 220 mm and a length of 110 mm. This rotating domain was situated inside a stationary rectangular domain, measuring 1.8 meters on each side and 2.25 meters in length. The arrangement of these domains can be observed in Figures 4a and 4b. This configuration allows for the rotation of the turbine during the transient simulation. The domains were sized to prevent the interference of the domain boundaries in the flow around the turbine while also providing plenty of space for the fluid mat to develop.

The mesh was built using the inflation and body of influence techniques in order to obtain a high-quality discretization of the fluid rotor interface and a great fidelity of the fluid mat before and after the turbine.

The mesh around the turbine rotor was generated with the inflation tool, this tool creates layers of tetrahedral mesh elements around the rotor surface to better capture the boundary layer effect on the blades of the rotor. The quality of the boundary layer has a major impact on the calculation of the local pressure applied on the blades, which impacts the torque at the turbine. The inflation was set as 10 levels with the first layer having a height of 10^-4. The layers can be seen in Figure 5.

The body of influence (BOI) technique was also used for the meshing, this tool allows for the creation of a more refined volume of mesh elements around a region of interest, in this case, the rotating domain and the fluid mat before and after the turbine. This region's refinement is important to achieve a higher precision at the velocity and pressure gradients for the flow. The BOI and the whole domain can be seen meshed in Figure 5.

A mesh convergence study was performed in order to evaluate when the size of the mesh becomes sufficiently good that its increase does not interfere with the torque calculated by the software. In order to conduct this study, a total of five meshes were created, employing the tools discussed before and reducing the element sizes to enhance accuracy. This refinement resulted in an increased number of elements and nodes within the meshes. Subsequently, the power coefficient was computed for the model 1.4 turbine at 1000 rpm using each mesh configuration. The resulting outcomes are presented in Table 2 below.

	Mesh Nodes	C_p
Mesh 1	0.4×10^6	0.166
Mesh 2	1.2×10^6	0.199
Mesh 3	3.5×10^6	0.232
Mesh 4	5.8×10^6	0.242
Mesh 5	7.5×10^6	0.236

Table 2: Flight parameters of the specimens collected

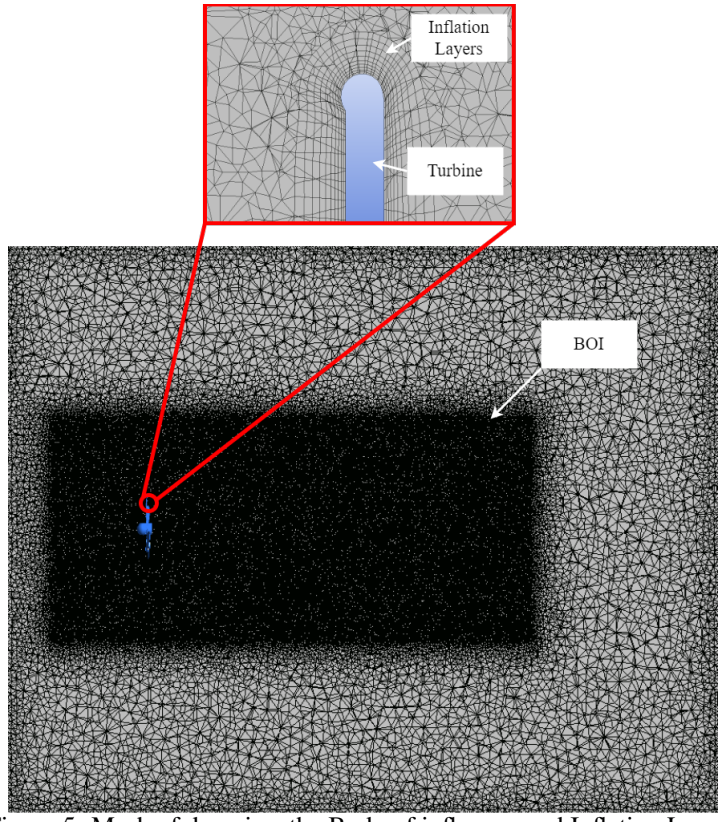

Figure 5: Mesh of domains, the Body of influence and Inflation Layers

The presented table demonstrates a remarkable 42% increase in the power coefficient when transitioning from the roughest mesh (mesh 1) to the more refined mesh (mesh 5), reaffirming the criticality of constructing a well-refined mesh. Additionally, it is worth noting that the calculated power coefficient for mesh 5 was slightly lower than that of mesh 4. It can be assumed that the mesh converged within the range of 5.8 to 7.5 million nodes, and the observed variation is attributed to the larger number of turbine rotations completed before and during the simulation with mesh 5. This increased fidelity of the flow led to a more accurate representation, resulting in a marginally lower power coefficient. all simulations presented further were performed with mesh 4.

The model is subject to the following boundary conditions. The sides of the static domain were assigned as openings, with a relative pressure of 0 atm. The front face of the static domain has the inlet condition with a normal velocity directed to the interior of the domain. The back face of the static domain has the outlet condition, with an absolute pressure of 0 atm. The simulations were performed with the Shear Stress Transport (SST) turbulence model selected due to its accurate results on the near-wall region. The boundary conditions as the whole domain are shown in Figure 6.

The simulation was initiated as a steady state simulation, and after 3 rotations of the turbine, converted into a transient simulation, when the data was saved. This option was made to reduce the time required to fully develop the fluid mat, resulting in faster simulations.

2.4 The power coefficient

The performance evaluation of the simulated turbines will be conducted based on the turbine's power coefficient (Cp). The power coefficient is a crucial metric for assessing the turbine's efficiency in harnessing the available kinetic energy from the wind. The power coefficient is defined as the extracted power over the available power, and its equation can be written as follows:

$$Cp = \frac{Torque \times 2 \times \pi \times \Omega}{\frac{1}{2} \times \rho \times A \times U_{\infty}^{3}} \tag{1}$$

Ω is the angular velocity of the turbine, A is the turbine's sweep area and U_{∞} is the wind velocity before the turbine interference. This formula can be used with the torque calculated by ANSYS CFX and used to verify which turbine performs the best in each scenario.

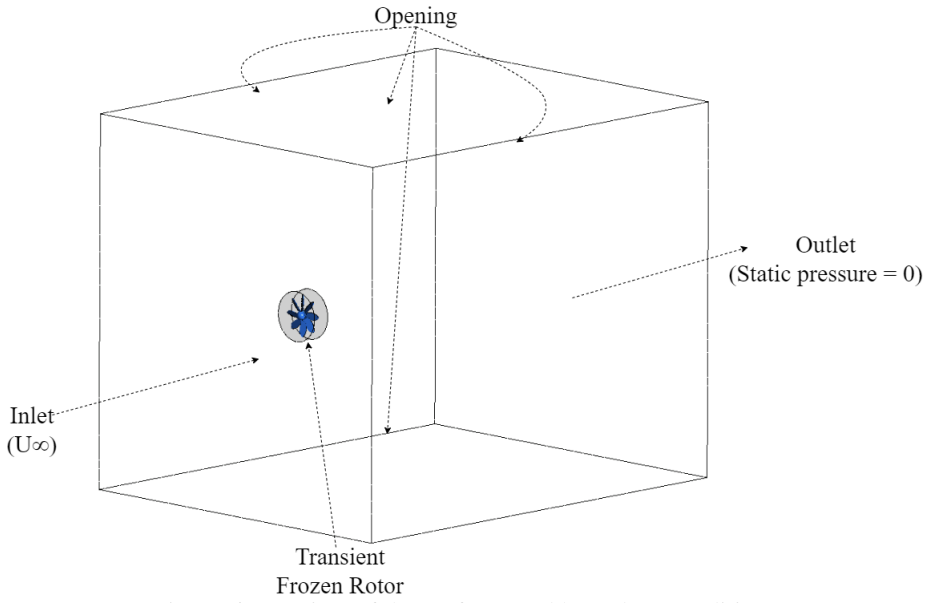

Figure 6: 3D view of the surfaces and boundary conditions.

3. RESULTS

3.1 Flight parameters obtained trough experiments

By performing the flight experiments with the samaras collected, as described in section 2.1, it was possible to collect the flight parameters of the *Pterogyne nitens* samaras. These parameters are shown in Table 3 below:

	Minimum	Maximum	Average	Standard Deviation
Falling velocity (m/s)	0.95	1.18	1.038	0.10
Angular velocity (rpm)	560	696	614.797	56.72
Tip speed (m/s)	2.558	3.721	2.849	0.49
Tip speed ratio	2.42	3.18	2.77	0.28
Flopping angle (°)	13.54	48.19	29.58	12.71

Table 3: Flight parameters of the specimens collected

The Falling velocity, Angular velocity, and Tip Speed variables were determined by measuring the displacement of the seed after a known interval of time (measured in frames). The tip speed ratio (TSR) was calculated according to Equation 2:

$$TSR = \frac{Tip\ speed}{Falling\ velocity} \tag{2}$$

In comparison to the Maple samara, our samaras exhibit a higher falling velocity at a lower angular velocity. Despite the maple seed having a higher angular velocity, our samaras maintain a similar tip speed due to their smaller length on the *Acer Diabolicum Blume*.

3.2 Turbine models and parameters influence

In order to build the best turbine model using the samaras geometry, multiple turbine models were built varying their blades' number or pitch angle, those models were simulated in the CFD software as described in the previous section.

The first generation of turbine models, with their characteristics and the calculated power coefficient, are shown in Table 4 below. To verify the influence of the blades' number, the pitch angle was fixed at 20°, and to verify the influence of the pitch angle, the blades' number was fixed at 5.

The table demonstrates the direct impact of the number of blades on the power coefficient, with an increase in the number of blades resulting in a corresponding increase in Cp. This goes in contrast to most turbine models, that have 2 or 4 blades, but is in accordance with previous studies about small or pico bio-inspired turbines, where a larger blade number was favorable for the turbine, as was the case for Carré *et al.* (2022).

Additionally, the pitch angle simulations revealed that the maximum performance was attained at a pitch angle of 30°.

Model	Blades Number	Blades' pitch angle (°)	Cp
1.1	3	20	0.83
1.2	4	20	0.12
1.3	5	20	0.14
1.4	6	20	0.16
1.5	7	20	0.17
1.6	5	5	0.04
1.7	5	10	0.08
1.8	5	30	0.17
1.9	5	40	0.14

Table 4: Turbine models simulated

Upon closer examination, we can notice that this angle aligns with the gliding angle observed in samaras. This correlation is logical as samaras naturally adapt to an optimal configuration during gliding.

Based on these findings, a second-generation model was developed, incorporating the optimal parameters from the first generation. The revised model features 8 blades and a pitch angle of 30°, as depicted in Figure 3. Further detailed simulations will be conducted using this model to explore its performance characteristics in depth.

3.3 Power coefficient x Tip spee dratio curve

To conduct a comprehensive analysis of the revised model, a detailed investigation was conducted. The turbine was subjected to simulations with angular velocities ranging from 700 to 1300 rpm. Following best practices, the results were plotted as a function of the tip speed ratio, yielding the graph depicted in Figure 7 below, for a wind speed of 10 m/s.

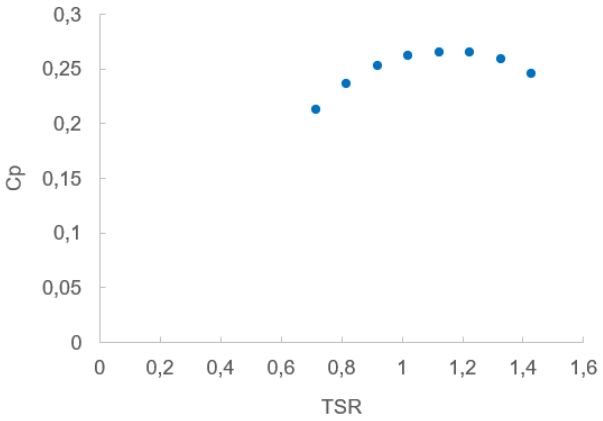

Figure 7: TSR x Cp curve for second generation model.

The optimum tip speed ratio for the turbine at a wind speed of 10 m/s is around 1.1 (1100 rpm), at which the power coefficient of the turbine is over 0.26. This value falls short of the maximum limit of 0.59 (known as the Betz limit for horizontal axis wind turbines), but it is considered a commendable outcome for a turbine with a diameter of 206 mm, as discussed in the conclusion section,

To assess the efficiency of the turbine at different wind speeds, the turbine was simulated for wind speeds of 6 to 12 m/s, with a constant angular velocity of 1000 rpm. The power coefficient as a function of the wind speeds is shown in Figure 8:

Based on the conducted simulations, it is evident that the turbine exhibits an increasing performance trend until reaching a wind speed of 10 m/s. Beyond this threshold, the performance starts to decline. This behavior can be attributed to the optimization efforts focused on the 10 m/s wind speed, as the pitch angle plays a critical role in determining the turbine's efficiency and is closely linked to the prevailing wind speed.

3.4 Flow visualisations

Figures 9 and 10 provide a qualitative representation of the simulation at 1000 rpm and 10 m/s, showcasing velocity levels and pressure gradients that demonstrate the physical consistency of the simulated outcomes. These figures reveal distinct hydrodynamic patterns associated with the flow over free axial machines. Notably, the flow behavior upstream of the machine remains consistent until the turbines come into proximity. The interaction between the rotor flow and the surrounding medium generates flow disturbances commonly referred to as a wake, which can be readily observed. The

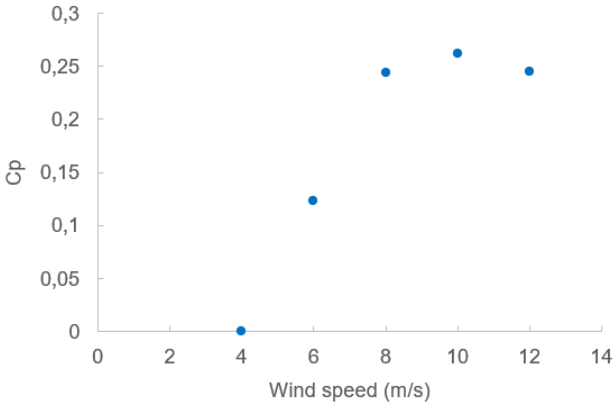

Figure 8: Wind speed x Cp curve for second generation model.

fluid downstream of the turbine experiences a significant decrease in velocity and an increase in turbulence. This can be attributed to the turbine's presence and its power extraction from the fluid.

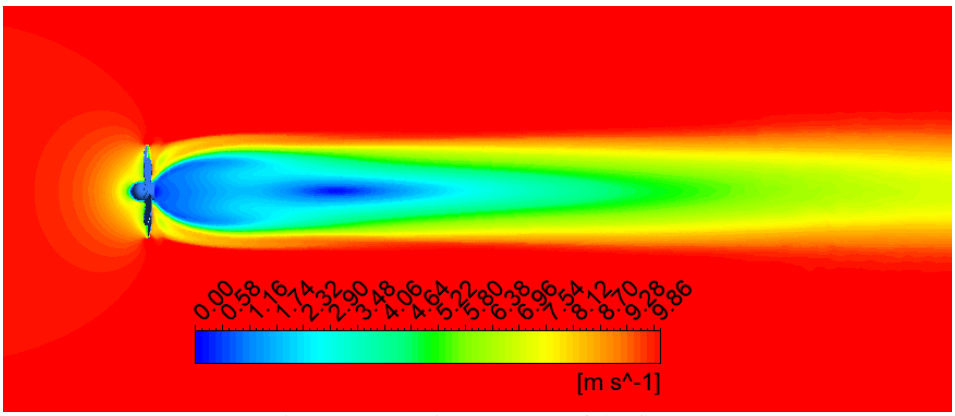

Figure 9: Velocity contours of the flow.

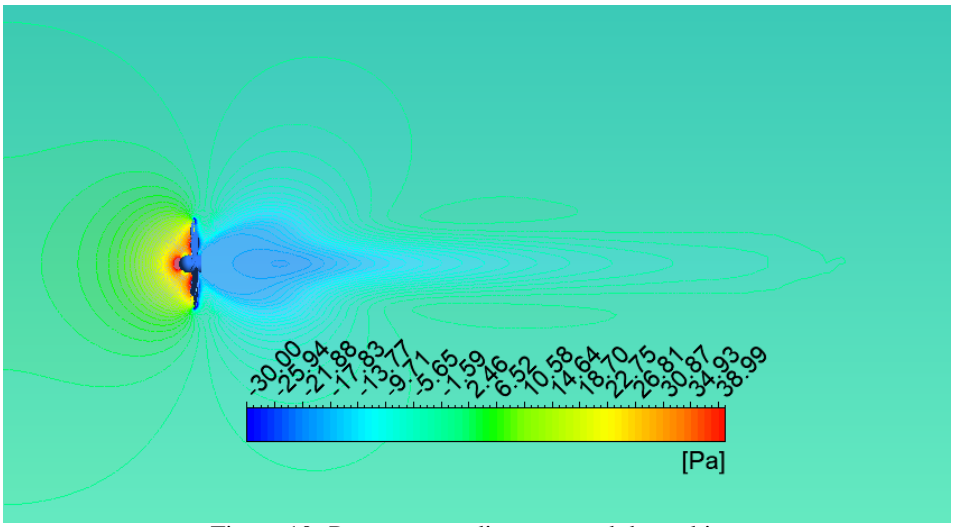

Figure 10: Preassure gradients around the turbine.

In terms of pressure levels, it is observed that there is an increase in pressure ahead of the turbine as a result of its presence, while a lower pressure is observed in the wake of the turbine. This pressure variation is expected and represents the power extraction by the turbine.

4. CONCLUSION

This study analyzes the flight of winged seeds from the *Pterogyne nitens* tree to develop bio-inspired wind turbines with blades that resemble the samaras geometry and simulate these turbines with a CFD software.

The experiments conducted with the winged seed specimens provided valuable insights into the flight characteristics and geometry of the samaras, allowing for a comparative analysis with existing literature on samaras. This study enhanced our understanding of the samaras' flight behavior and their similarities and differences with other documented samaras.

The culmination of developing multiple turbines and conducting simulations resulted in the creation of a turbine with a maximum power coefficient of 0.26.

The overall performance of the designed turbines can be compared to that of the HK10 turbine developed by the same laboratory of this study but using more conventional blade approaches Brasil Junior *et al.* (2017). In the HydroK project, the HK10 turbine achieved a maximum Cp of 0.25 in wind tunnel testing at a scale model with dimensions similar to the turbines in this study. This value is similar to the Cp achieved here, which demonstrates the effectiveness of samara geometry to interact with the wind despite the absence of common design features like airfoil design or blade twist and generate torque. The findings indicate that samaras hold potential as wind turbine blades for efficient power extraction.

5. ACKNOWLEDGEMENTS

The Laboratório de Energia e Ambiente of the Universidade de Brasília for the technical support.

6. REFERENCES

Arranz, G., Moriche, M., Uhlmann, M., Flores, O. and García-Villalba, M., 2018. "Kinematics and dynamics of the auto-rotation of a model winged seed". *Bioinspiration Biomimetics*, Vol. 13. doi:10.1088/1748-3190/aab144.

Azuma, A. and Yasuda, K., 1989. "Flight performance of rotary seeds". *Journal of Theoretical Biology*, Vol. 138, No. 1, pp. 23–53. ISSN 0022-5193. doi:https://doi.org/10.1016/S0022-5193(89)80176-6. URL `https://www.sciencedirect.com/science/article/pii/S0022519389801766`.

Brasil Junior, A.C.P., Mendes, R.C.F., Lacroix, J., Noguera, R. and Oliveira, T.F., 2017. "Hydrokinetic propeller turbines. How many blades?" *American Journal of Hydropower, Water and Environment Systems*, Vol. 2, pp. 16–23. doi: 10.14268/ajhwes.2017.00039.

Carré, A., Gasnier, P., Roux, E. and Tabourot, L., 2022. "Extending the operating limits and performances of centimetre-scale wind turbines through biomimicry". *Applied Energy*, Vol. 326, p. 119996. doi:10.1016/j.apenergy.2022.119996.

Gaertner, E., Rinker, J., Zahle, L.S.F., Anderson, B., Barter, G., Abbas, N., Meng, F., Bortolotti, P., Skrzypinski, W., Scott, G., Feil, R., Bredmose, H., Dykes, K., Shields, M., Allen, C. and Viselli, A., 2020. "Definition of the iea wind 15-megawatt offshore reference wind turbine (technical report)". doi:https://www.nrel.gov/docs/fy20osti/75698.pdf.

Holden, J., Caley, T. and Turner, M., 2015. "Maple seed performance as a wind turbine". doi:10.2514/6.2015-1304.

IEA, 2022. "Wind electricity". doi:https://www.iea.org/reports/wind-electricity.

Ikeda, T., Tanaka, H., Yoshimura, R., Noda, R., Fujii, T. and Liu, H., 2018. "A robust biomimetic blade design for micro wind turbines". *Renewable Energy*, Vol. 125, pp. 155–165. ISSN 0960-1481. doi:https://doi.org/10.1016/j.renene.2018.02.093. URL `https://www.sciencedirect.com/science/article/pii/S0960148118302374`.

LJ, F., Hand, M. and AS, L., 2006. "Wind turbine design cost and scaling model". doi:10.2172/897434.

Sathyajith, M. and Philip, G., 2011. *Advances in Wind Energy Conversion Technology*. ISBN 978-3-540-88257-2. doi: 10.1007/978-3-540-88258-9.

7. RESPONSIBILITY NOTICE

The author(s) is (are) the only responsible for the printed material included in this paper.